Pediatr Radiol (2012) 42:418–430
DOI 10.1007/s00247-011-2278-x

ORIGINAL ARTICLE

^{18}F-FDG PET/CT compared to conventional imaging modalities in pediatric primary bone tumors

Kevin London · Claudia Stege · Siobhan Cross · Ella Onikul · Nicole Graf · Gertjan Kaspers · Luciano Dalla-Pozza · Robert Howman-Giles

Received: 7 April 2011 / Revised: 27 July 2011 / Accepted: 9 August 2011 / Published online: 2 December 2011

Abstract
Background F-Fluoro-2-deoxy-D-glucose (FDG) positron emission tomography (PET) is useful in adults with primary bone tumors. Limited published data exist in children.
Objective To compare hybrid FDG positron emission tomography/computed tomography (PET/CT) with conventional imaging (CI) modalities in detecting malignant lesions, predicting response to chemotherapy and diagnosing physeal involvement in pediatric primary bone tumors.
Materials and methods Retrospective analysis of PET/CT and CI reports with histopathology or follow-up>6 months as reference standard. Response parameters and physeal involvement at diagnosis were compared to histopathology.
Results A total of 314 lesions were detected in 86 scans. Excluding lung lesions, PET/CT had higher sensitivity and specificity than CI (83%, 98% and 78%, 97%, respectively). In lung lesions, PET/CT had higher specificity than CI (96% compared to 87%) but lower sensitivity (80% compared to 93%). Higher initial SUV_{max} and greater SUV_{max} reduction on PET/CT after chemotherapy predicted a good response. Change in tumor size on MRI did not predict response. Both PET/CT and MRI were very sensitive but of low specificity in predicting physeal tumor involvement.
Conclusion PET/CT appears more accurate than CI in detecting malignant lesions in childhood primary bone tumors, excluding lung lesions. It seems better than MRI at predicting tumor response to chemotherapy.

Keywords Osteosarcoma · Ewing sarcoma · Bone neoplasm · FDG · Positron emission tomography

K. London (✉) · R. Howman-Giles
Department of Nuclear Medicine,
The Children's Hospital at Westmead,
Sydney, NSW, Australia
e-mail: kevinL5@chw.edu.au

K. London
Discipline of Paediatrics and Child Health,
Sydney Medical School, University of Sydney,
Sydney, NSW, Australia

C. Stege · G. Kaspers
Divisions of Paediatric Oncology/Haematology,
VU Medical Centre,
Amsterdam, The Netherlands

S. Cross · L. Dalla-Pozza
Department of Oncology, The Children's Hospital at Westmead,
Sydney, Australia

E. Onikul
Department of Medical Imaging,
The Children's Hospital at Westmead,
Sydney, Australia

N. Graf
Department of Pathology, The Children's Hospital at Westmead,
Sydney, Australia

R. Howman-Giles
Discipline of Imaging, Sydney Medical School,
University of Sydney,
Sydney, NSW, Australia

Introduction

Primary bone tumors make up 5–6% of childhood and adolescent malignancies, with the majority being osteogenic sarcoma (OS) and Ewing sarcoma (ES) [1].

Important considerations for determining prognosis and subsequent management include tumor histology and grade, the location of the primary tumor, the extent of loco-regional and metastatic disease, and response to chemotherapy [2]. The extent of loco-regional disease is usually defined on MRI

[3]; however, these tumors, particularly in the Ewing group, demonstrate a variable degree of adjacent soft tissue abnormality that can make assessment of the extent of the primary tumor difficult. PET/CT imaging using the glucose analogue ^{18}F-fluoro-2-deoxy-D-glucose (FDG) may provide relevant ancillary information to conventional imaging (CI) and identify more accurately the extent of disease at diagnosis.

Response of the primary tumor to chemotherapy is not assessed accurately by MRI [4]. FDG PET/CT has the potential to provide a non-invasive, in vivo imaging technique to evaluate tumor necrosis and provide an opportunity to identify children likely to benefit from further adjuvant therapy before surgery.

Studies in adults with primary bone and soft tissue sarcomas confirm the accuracy of FDG PET/CT in the detection of malignant lesions [5, 6], assessing histological response to chemotherapy [7] and predicting survival [8, 9]. Studies have also been published that incorporate children with bone and soft tissue sarcomas and show FDG PET/CT to be clinically useful, provide additional information to CI and alter management [10, 11], but evidence from childhood studies is lacking.

Our aims were to evaluate the performance of FDG PET/CT compared to CI in detecting malignant lesions, predicting histological response to chemotherapy and diagnosing physeal involvement in children with primary bone tumors.

Materials and methods

Subjects

The electronic database of all PET/CT scans performed at the Children's Hospital at Westmead, Sydney, Australia during the period June 2006 to December 2008 was searched to identify all children with OS and ES. The histologic diagnoses were confirmed and imaging reports and histopathological results following surgery were analyzed retrospectively. To be eligible for inclusion, correlative CI (CT, US, MRI and/or bone scintigraphy) of lesions was required within 4 weeks of PET/CT, and clinical follow-up for at least 6 months after PET/CT.

PET/CT technique and analysis

PET/CT scans were carried out using a Siemens Biograph16 HiRez PET/CT system (Siemens Medical Solutions, Erlangen, Germany). All children fasted for 4–6 h before injection of 370 MBq (scaled to weight) of FDG and had blood glucose levels within the normal range. During the uptake phase, the children rested in a warm, dimly lit room lying down with minimal stimulation. Acquisition time was 2 min per 16 cm axial field of view for whole-body imaging.

PET/CT scans at our institution are reported after review by two pediatric nuclear medicine physicians trained in PET/CT interpretation. All relevant CI and clinical information are available at the time of reporting. Lesions reported as positive, suggestive, or equivocal for malignancy were considered positive for the analysis.

For the purpose of our study, if the reported findings were ambiguous, then PET/CT scans were reviewed by a pediatric nuclear medicine physician (R.H.G., 35 years of experience or K.L., 4 years of experience) to determine the final classification of lesions.

CI evaluation and analysis

CI was performed according to the patient's clinical requirement and consisted of CT, US, MRI, and/or bone scintigraphy. Studies reported as positive, suggestive, or equivocal for malignancy were considered positive for the analysis.

If the reported findings were ambiguous, then CI scans were reviewed by a pediatric radiologist (E.O., 21 years of experience) to determine the final classification of lesions.

Comparison of PET/CT and CI

A lesion-based analysis was used to determine the performance of PET/CT and CI in detecting malignant lesions. Imaging performed at diagnosis, at completion of treatment and during routine surveillance was included. Findings for PET/CT and CI were each compared to a defined reference standard. The reference standard was histopathological evaluation, if available. If lesion histopathology was not

Table 1 Primary tumor site and histopathological type. *OS* Osteogenic sarcoma, *ES* Ewing sarcoma

Primary tumor site	Number of children by tumor type	
	OS	ES
Femur	12	–
Tibia	5	3
Rib	–	6
Pelvis/sacrum	1	4
Spine	–	3
Nasal bone	–	1
Base of skull	–	1
Mandible	–	1
Humerus	1	–
Radius	1	–
Ulna	–	1
Fibula	–	1
Totals	20	21

Table 2 Lesion-based ^{18}F-fluoro-2-deoxy-D-glucose (FDG)-PET/CT and conventional imaging (CI) in the diagnosis of malignant lesions. *TP* True positive, *TN* true negative, *FP* false positive, *FN* false negative

		TP	TN	FP	FN
All lesions included	PET/CT	27	274	7	6
	CI	28	265	16	5
Excluding lung lesions	PET/CT	15	206	4	3
	CI	14	203	7	4
Lung lesions	PET/CT	12	68	3	3
	CI	14	62	9	1

performed, further imaging combined with clinical follow up for at least 6 months was used to determine the lesion reference standard classification. For example, in the case of a child entering remission, lesions that resolved on follow-up imaging were considered malignant and lesions that remained stable or progressed were considered non-malignant. In the case of a child experiencing disease progression, lesions that progressed were considered malignant and lesions that resolved or remained stable on follow-up imaging were considered non-malignant.

PET/CT and MRI performed at diagnosis and following neo-adjuvant chemotherapy before surgery were analyzed to determine the ability of these modalities to predict histological response of the primary tumor. PET/CT was aimed to be performed at least 3 weeks after the last dose of chemotherapy. Semi-quantitative assessment of primary tumor FDG uptake was performed by calculation of maximum standardised uptake value (SUV_{max}) using a volumetric analysis tool (Siemens ESOFT workstation, Erlangen, Germany). An ellipsoid volume of interest was placed manually encompassing the primary tumor and the SUV_{max} at diagnosis and following chemotherapy were recorded. On MRI in the coronal plane, the maximal cranio-caudal diameter ($diameter_{CC}$) and maximal transverse diameter ($diameter_T$) of the primary tumor was recorded. If this data was not available on the scan reports, the MRI was reviewed by a pediatric radiologist (E.O.) and the tumor measurements were taken. The maximal cross sectional area (CSA_{max}) at diagnosis and following chemotherapy was calculated according to the formula $CSA_{max} = diameter_{CC} \times diameter_T$.

SUV_{max} at diagnosis, and the change in SUV_{max} and CSA_{max} following chemotherapy were compared to histopathologic evaluation of viable tumor after en block primary tumor resection after chemotherapy. The change in SUV_{max} and CSA_{max} were expressed as a ratio of these parameters after chemotherapy to before chemotherapy. Less than 10% residual viable tumor was used to classify the response as "good" and greater than or equal to 10% residual viable tumor was used to classify the response as "poor".

The children with primary tumors involving metaphyses were identified and the reported involvement of the physis on PET/CT and MRI was recorded. If physeal involvement was not commented on specifically in the imaging reports, the scans were reviewed (PET/CT by R.H.G., MRI by E.O.) for final classification. Imaging findings were compared to histopathologic evaluation of physeal involvement following en block resection of the primary tumor after chemotherapy.

Statistical analysis

Standard 2 × 2 tables were constructed of the relevant data. Sensitivity, specificity, accuracy and positive likelihood ratio (PLR) were calculated; 95% confidence intervals for each parameter were calculated using an online calculator adhering to standard statistical methods [12]. A non-parametric test for statistical difference (Mann-Whitney-U test) with alpha=0.05 was used to compare predictors of treatment response (SUV_{max} data and CSA_{max} data) between FDG PET/CT and CI. Statistical computer software was used for the analysis (SPSS version 19, IBM). No statistical analysis was performed on the data for predicting physeal involvement due to the very small number of children included in this evaluation.

Ethical approval for the study was obtained from The Human Research Ethics Committee of The Children's Hospital at Westmead.

Table 3 Diagnostic performance of FDG-PET/CT and CI in detecting malignant lesions. Values are expressed as percentages with 95% confidence intervals. *PLR* Positive likelihood ratio

		Sensitivity, %	Specificity, %	Accuracy, %	PLR
All lesions included	PET/CT	81.8 (63.9-92.4)	97.5 (94.7-98.9)	95.9 (92.9-97.7)	32.8 (15.5-69.5)
	CI	84.8 (67.3-94.3)	94.3 (90.7-96.6)	93.3 (89.8-95.7)	14.9 (9.1-24.5)
Excluding lung lesions	PET/CT	83.3 (57.5-95.6)	98.1 (94.9-99.4)	96.9 (93.5-98.6)	44.0 (16.3-118.6)
	CI	77.8 (51.9-92.6)	96.7 (93.0-98.5)	95.2 (91.3-97.4)	23.3 (10.8-50.3)
Lung lesions	PET/CT	80.0 (51.3-94.6)	95.8 (87.3-98.9)	93.0 (84.8-97.1)	18.9 (6.1-58.9)
	CI	93.3 (66.0-99.6)	87.3 (76.8-93.6)	88.4 (79.2-93.9)	7.4 (3.9-13.8)

Results

A total of 155 PET/CT scans in 41 children (26 male) with OS (n=20) and ES (n=21) with an average age at the time of the scan of 12.7 years (range, 1.8 years–18.7 years), had been performed during the review period. In total, 616 lesions were identified on PET/CT and/or CI; 16 scans were performed at diagnosis, 2 at relapse, 24 during therapy, 14 at the end of therapy and 99 during routine surveillance. In total there were 12 different primary tumor sites (Table 1). Eight children had metastatic disease at time of diagnosis: four with lung metastases, one with a bone metastasis and three with both lung and bone metastases.

In all, 49 scans (248 lesions) in eight children were excluded due to follow-up of less than 6 months (42 scans) or no corresponding CI within 4 weeks of the PET/CT (7 scans). There remained 106 scans (368 lesions) in 33 children eligible for inclusion in the study, of which 86 scans (314 lesions) in 33 children were used for assessing diagnostic accuracy (performed at diagnosis, at completion of treatment and during routine surveillance).

Diagnostic accuracy

The individual lesion-based results are shown in Table 2. The sensitivity, specificity, accuracy and PLRs with corresponding 95% confidence intervals for PET/CT and CI are presented in Table 3.

Overall, 14/86 (16%) of the scans had at least one lesion with discordant PET/CT and CI findings and 22/314 (7.0%) of the total lesions detected had discordant PET/CT and CI findings. PET/CT was correct in 15 of these 22 (68%). The

Table 4 Lesion-based false negative findings at FDG-PET/CT and CI

Clinical background	Scan indication	PET/CT false negative lesions	CI false negative lesions	Comments
Previously treated proximal fibula ES	Surveillance	Lung lesions not seen	Interpreted as infectious lung nodules	Fluffy nodules in left lower lobe on CT scan considered infective in nature. Biopsy after further follow-up (next row) showed recurrent ES
	Surveillance	7-mm lung nodule not seen 4-mm lung nodule not seen	— —	More discrete nodules seen on diagnostic CT scan in same area as previously (row above). Biopsy-proven ES
Distal femur OS with multiple bone and lung metastasis	Staging	—[a]	Proximal tibial metastasis not seen	Tibial lesion not seen on MRI, but seen on PET/CT. Proven to be metastasis (see Fig. 1)
		Femoral shaft metastasis not seen	—	Presumed skip metastases seen on MRI but not seen on PET/CT. Resolved on subsequent MRI following treatment
Previously treated proximal humerus OS	Surveillance	Primary site recurrence not detected	Primary site recurrence not detected	FDG-uptake at proximal humerus thought to be reactive due to joint prosthesis. No evidence of recurrence on diagnostic CT; 2 months later biopsy-proven local recurrence
Distal femoral OS with skeletal and lung metastases	Staging	—	Bone marrow	Focal abnormal FDG-uptake in bone marrow of vertebral bodies. Diagnostic CT normal. FDG appearance resolved after successful therapy
Previous tibial OS, treated for isolated pulmonary relapse	End of therapy	Brain recurrence not detected	Brain recurrence not detected	Brain MRI showed a left frontal lobe lesion considered to be an area of gliosis attributed to previous therapy. PET/CT showed corresponding mildly reduced FDG uptake; 5 months later, extensive relapse involving left frontal lobe and multiple skeletal and lung metastases (see Fig. 2)

[a] Malignant lesion detected

Table 5 Description of the lesion-based false positive findings at FDG-PET/CT and C)

Clinical background	Scan indication	PET/CT false positive lesions	CI false positive lesions	Comments
Treated isolated lung recurrence of OS	End of therapy	FDG uptake in fibrotic lung lesion	—[a]	FDG-avid lesion in right upper lobe. Stable in size on serial diagnostic CT scans and thought to represent fibrosis. Biopsy proven benign fibrovascular tissue
Previously treated sacral ES	Surveillance	FDG-uptake in piriformis muscle	—	Focal FDG-uptake in left piriformis muscle. MRI scan showed changes consistent with previous radiotherapy. Biopsy proven normal skeletal muscle
Distal femur OS	Staging	—	Bone scan positive scapula	Focal tracer uptake on bone scan in spina of right scapula. No increased FDG-uptake; 10 months after successful therapy, bone scan appearance persisted. Attributed to a benign stress reaction
Treated distal femoral OS	End of therapy	FDG uptake in pleural lesion	Pleural lesion	New FDG-avid left pleural lesion and right lower lobe lesions. Unsuccessful diagnostic CT-guided biopsy but lesions resolved with antibiotic therapy. Attributed to septic emboli related to an infected central venous catheter
		FDG uptake in right lower lobe	Rounded densities right lower lobe	
		—	Right middle lobe poorly defined increased density lesions	New lung lesions seen on diagnostic CT but not on PET/CT. Subsequently attributed to infective emboli as above and resolved with antibiotic therapy
		—	Left lower lobe poorly defined increased density lesions	
		—	20-mm left iliac lymph node	Left iliac lymphadenopathy seen on diagnostic CT, considered a benign reactive lymph node on PET/CT. Resolved on subsequent imaging without further cancer directed treatment
Previously treated spinal ES	Surveillance	—	3-mm right middle lobe nodule	New lung nodules seen on diagnostic CT but not on PET/CT. Resolved on follow up imaging without further cancer treatment
		—	Left lower lobe subpleural nodule	
Previously treated pelvic ES	Surveillance	—	13-mm right axilla lymph node	Right axilla lymphadenopathy seen on diagnostic CT scan. Considered a benign reactive cause on PET/CT. Follow up on subsequent scans
	Surveillance	—	15-mm right axilla lymph node	Follow-up CT scan showed increasing right axillary lymphadenopathy but remaining FDG negative. Attributed to a reactive cause related to a skin infection and resolved on follow up imaging without further cancer directed treatment
Previously treated tibial ES	Surveillance	Seen on attenuation CT, no FDG-uptake	5-mm left lower lobe nodule	New lung nodule seen on diagnostic CT. Same lesion seen on PET/CT and although not FDG avid was considered suspicious for recurrence. Subsequently resolved on follow up imaging without further cancer directed treatment
Proximal tibial ES	Staging	Moderate FDG-uptake left femoral lymph node	—	Increased FDG-uptake seen in small left femoral and inguinal lymph nodes. Not considered abnormal on CT. Biopsy-proven reactive and attributed to an infection at the primary tumor biopsy site
		Moderate FDG-uptake left inguinal lymph node	—	
		—	3-mm right lower lobe nodule	Small bilateral lung nodules seen on CT. Not seen on PET/CT. Biopsy confirmed benign reactive subpleural lymph nodes
		—	3-mm left lower lobe nodule	

Table 5 (continued)

Clinical background	Scan indication	PET/CT false positive lesions	CI false positive lesions	Comments
Previously treated 4th rib ES	Surveillance	—	Subscapularis rim enhancing lesion	MRI showed an enhancing lesion anterior to the subscapularis muscle. Not FDG-avid. Resolved on further imaging without cancer treatment. Attributed to a trauma-related seroma (see Fig. 3)
	Surveillance	—	Ill-defined left upper lobe nodule	New left lung nodule seen on CT. Not seen on PET/CT. Resolved on further imaging without cancer treatment
Treated chest wall ES	End of therapy	—	Right pleural effusion	New pleural effusion seen on CT. Not FDG-avid. Subsequently resolved on follow-up imaging without cancer treatment Attributed to a benign reactive effusion related to therapy

[a] Lesion correctly not identified as malignant

lesions diagnosed incorrectly on PET/CT and/or CI are described in Table 4 (the false negative findings) and Table 5 (the false positive findings) and in Figs. 1, 2 and 3.

Tumor response to chemotherapy

Seventeen children had PET/CT for disease staging at diagnosis or relapse before therapy. SUV_{max} at initial diagnosis ranged from 5.3 to 42.8 (mean 12.2, median 8.2).

For the evaluation of PET/CT parameters in predicting histological response of the primary tumour, nine children were excluded: two for restaging of lung relapse, two without PET/CT performed after chemotherapy and five with histopathology not available or not performed (one base of skull tumor, two pelvic tumors, one rib relapse, one who refused surgery). The eight children remaining were included in the analysis. Of these eight, six had good and two poor response (Table 6). Examples of PET/CT and

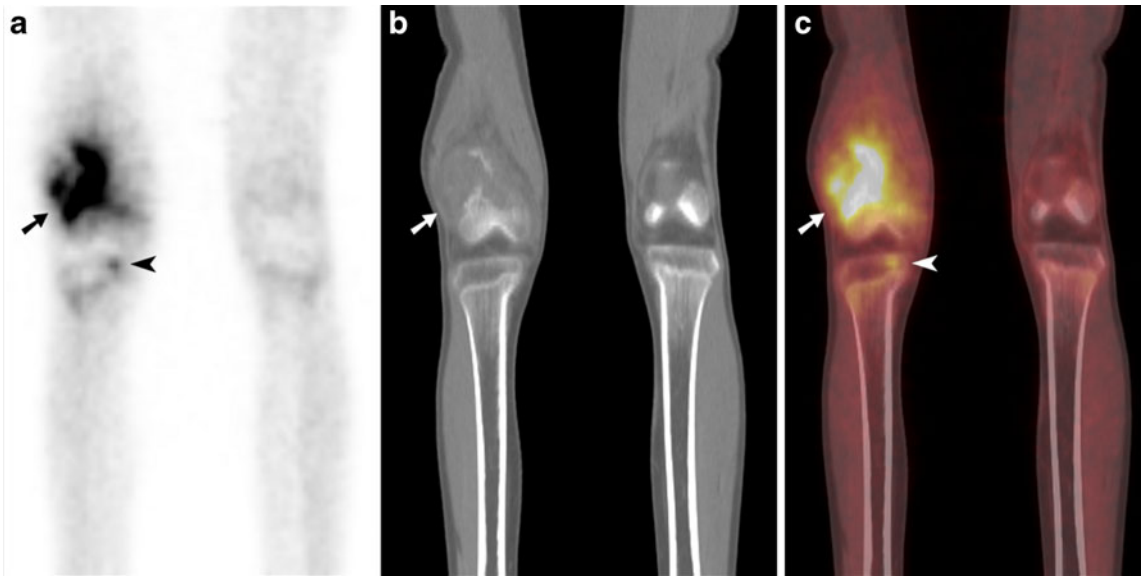

Fig. 1 Example of a discordant conventional imagine (CI) false negative lesion. **a** Staging ^{18}F-fluoro-2-deoxy-D-glucose (FDG) PET, **(b)** corresponding low dose attenuation CT, and **(c)** fused PET/CT of a 13-year-old boy with osteogenic sarcoma (OS). Intense FDG uptake with disrupted bone cortex and soft tissue is seen involving in the primary tumor site in the right distal femur (*arrow*). There is also a small intense focus of increased FDG uptake in the right proximal tibial epiphysis medially (*arrowhead*), without abnormality seen on the low dose attenuation CT scan. No abnormality was seen on the MRI scan in the right proximal tibia (image not shown). A metastasis in the right proximal tibial epiphysis was confirmed by histopathology following surgery

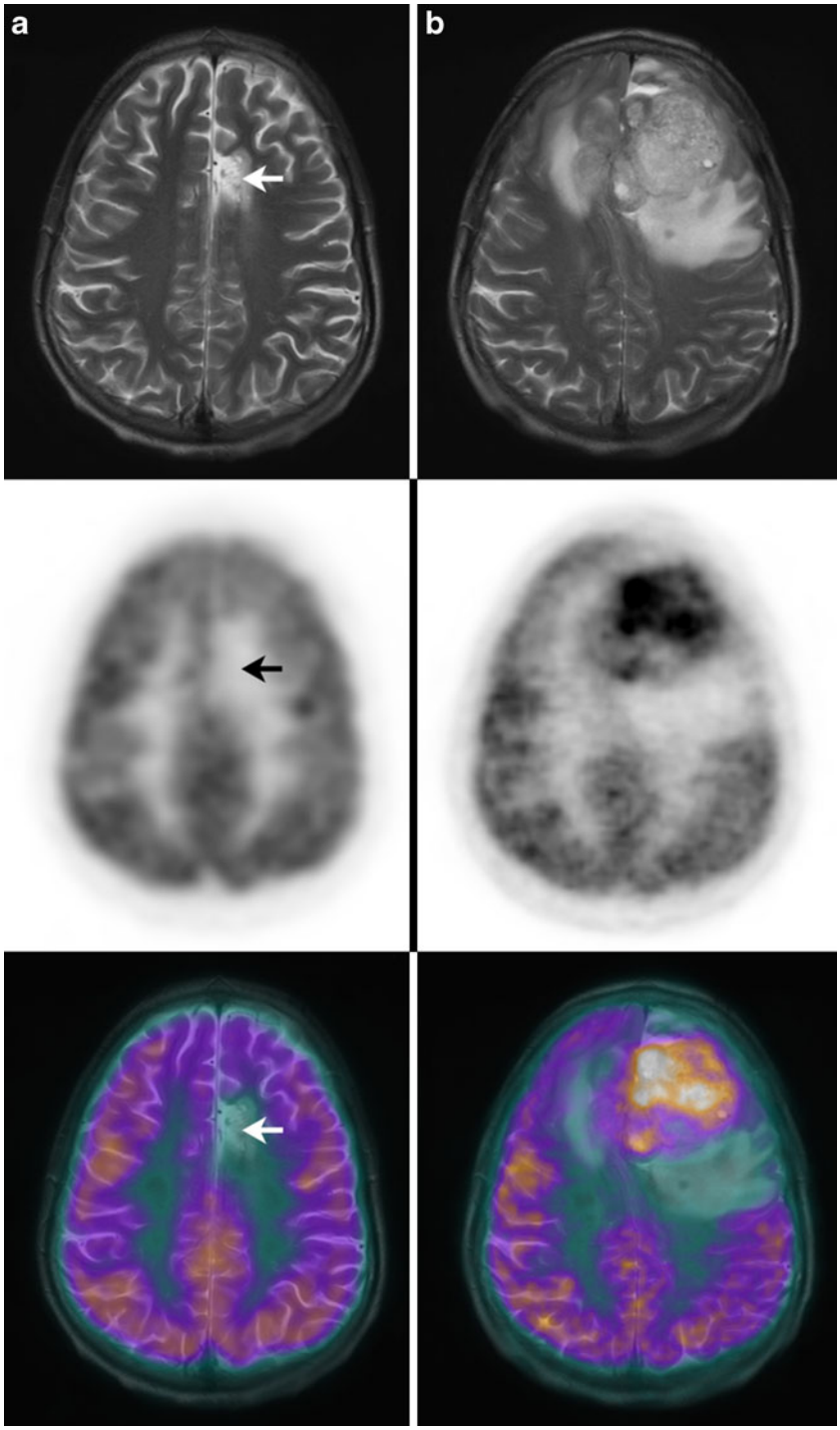

Fig. 2 Example of a concordant PET/CT and CI false negative lesion. Cerebral T2 weighted MRI (upper row), FDG PET (middle row) and fused co-registered PET/MRI (lower row) of a 17-year-old boy performed at two time points following therapy for pulmonary relapse of right tibial osteogenic sarcoma. The child had a transient encephalopathy attributed to a side effect of chemotherapy prompting the cerebral imaging. **a** (*left panels*) Initial imaging showed a high signal abnormality in the parasagittal anterior left frontal lobe (*arrow*) thought to represent an area of gliosis and atrophy associated with previous therapy. The FDG PET and fused co-registered PET/MRI show the lesion to be relatively hypometabolic (*arrow*). **b** (*right panels*) Follow up imaging performed 6 months later shows the development of a large hypermetabolic lesion in the left frontal lobe. There were also pulmonary and multiple skeletal metastases (images not shown)

MRI imaging of good and poor response are shown in Figs. 4 and 5, respectively.

SUV_{max} values at diagnosis and after chemotherapy were available for all eight children. There was a trend for SUV_{max} at diagnosis to be higher in those tumors that responded well (median, 14.5) than in those with a poor response (median, 8.0; P=0.096). In all children, SUV_{max} was reduced following chemotherapy. However, tumors with good response appeared to have a greater reduction in SUVmax with a median ratio post/pre of 0.24, compared to 0.55 in the poorly responding tumors (P=0.18). The largest SUV_{max} decrease was found in the lesion with the highest initial SUV_{max} (Table 6).

CSA_{max} values were not available for one of the well-responding tumors due to MRI scans being performed at another institution. Seven children were included in the MRI analysis, five with good response and two with poor response to chemotherapy. There was no consistent pattern of change in size of the primary tumor seen on MRI

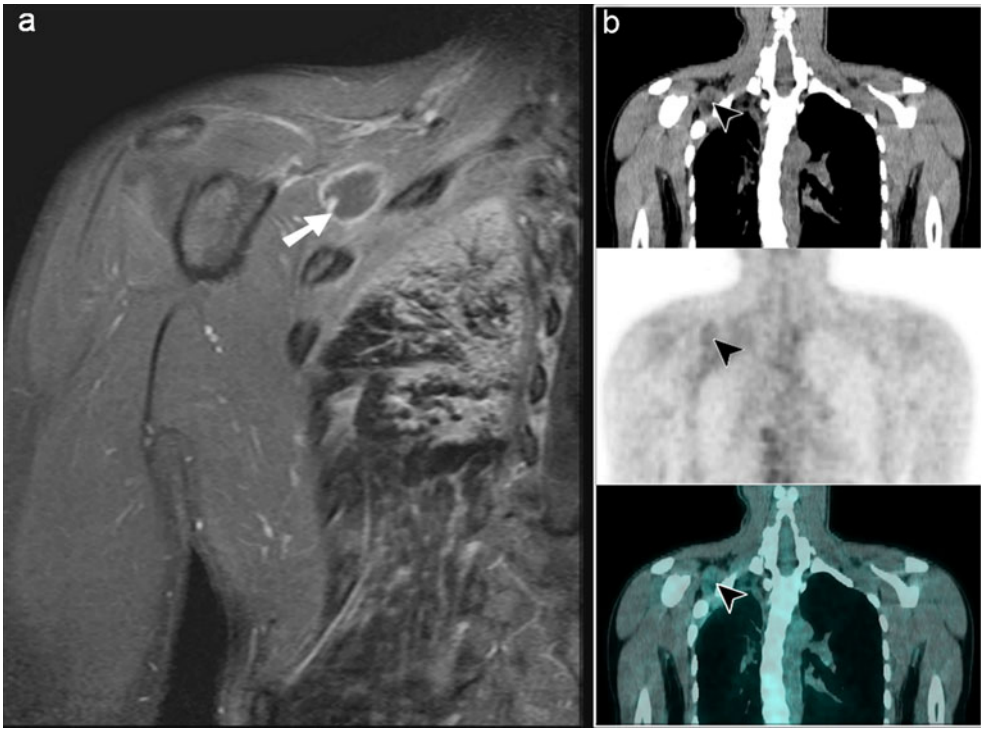

Fig. 3 Example of a CI false positive PET true negative lesion in a 15-year-old girl with previous Ewing sarcoma (ES) of the right 4th rib treated with rib excision, chemotherapy and radiotherapy. **a** During surveillance, an MRI scan showed a 2.5 cm rim-enhancing fluid-containing lesion anterior to the subscapularis muscle (*arrow*) thought to potentially represent relapse. **b** At the same time, FDG PET/CT showed the lesion to have very low level tracer uptake (*arrowhead*)—not greater than mediastinal blood pool. The lesion resolved on further imaging without cancer-directed therapy and was attributed to a trauma-related seroma

between the response groups. Two tumors with good response increased in size and three reduced in size. Both tumors with poor response reduced in size (Table 6).

Assessment of physeal involvement

Assessment of physeal involvement (Table 7), revealed that six children had a primary tumor in an extremity, involving the metaphysis, had documented histopathological assessment including the physis, and had complete PET/CT and MRI data available. All of these appeared to have physeal involvement on PET/CT (two false positives) compared to five children on MRI (one false positive). The child without physeal involvement on MRI had concordant histopathological assessment. An example of PET/CT and MRI imaging in evaluation of physeal involvement is shown in Fig. 6.

Discussion

Our study of children with primary bone tumors showed that FDG-PET/CT had higher specificity but lower sensitivity in detection of malignant lesions when all lesions were considered. The reduced sensitivity of PET/CT was most apparent in the assessment of lung lesions, with the three out of six false negative PET/CT-lesions being lung lesions<10 mm in diameter. CI (here, chest CT), while being more sensitive, had a considerably lower specificity with a higher rate of false positive findings in the lungs. Of the 16 false positive lesions seen on CI, 10 were small parenchymal lung lesions. Our findings are consistent with studies of osteosarcoma in adults and with studies of solitary pulmonary nodules in general [13, 14]. There is likely a combination of explanatory factors, including lung nodules below the limit of resolution of PET/CT, partial volume effects and respiratory movement. High-resolution chest CT remains the most sensitive tool for small nodules. The higher specificity of FDG PET/CT reinforces the complementary roles of these imaging modalities in the assessment of lung lesions (Fig. 7).

With the exclusion of lung lesions, PET/CT was both more sensitive and specific than CI for malignant lesions. Positive and negative predictive values have an intimate reliance on the disease prevalence in the study population and therefore may not be applicable to populations with a different underlying risk of disease. PLRs are a way to express the overall usefulness of a diagnostic test to confirm the presence of a disease that combines both test sensitivity and specificity, and is independent of the disease prevalence in the underlying study population [15]. In general, a PLR>10 indicates a conclusive increase in the probability of having the disease [16]. Our results show very high PLRs for both PET/CT (44.7) and CI (24.2) in evaluating lesions outside of the lungs. For lung lesions, CI had a lower PLR (7.4) in the "moderately useful" range [16]. This was due to the high false-positive rate. PET/CT however maintained a very high PLR (19.2) for assessing lung lesions despite the lower sensitivity, indicating that when positive, it is a more useful than CI.

Morphological assessment by plain radiographs and MRI following neoadjuvant chemotherapy is insufficiently

Table 6 Children included in the analysis of tumor response to chemotherapy. $SUV_{max}1$ Maximum standardized uptake value at diagnosis, $SUV_{max}2$ maximum standardized uptake value after chemotherapy, $Diameter_{CC}1$ maximal cranio-caudal diameter at diagnosis, $Diameter_T1$ maximal transverse diameter at diagnosis, $CSA_{max}1$ maximal cross sectional area at diagnosis, $Diameter_{CC}2$ maximal cranio-caudal diameter after chemotherapy, $Diameter_T2$ maximal transverse diameter after chemotherapy, $CSA_{max}2$ maximal cross sectional area after chemotherapy

Background			PET/CT			MRI at diagnosis			MRI after chemotherapy				Histopathology	
Age (years)	Sex	Diagnosis	Primary tumor site	$SUV_{max}1$	$SUV_{max}2$	$SUV_{max}2$: $SUV_{max}1$	$Diameter_{CC}1$ (cm)	$Diameter_T1$ (cm)	$CSA_{max}1$ (cm^2)	$Diameter_{CC}2$ (cm)	$Diameter_T2$ (cm)	$CSA_{max}2$ (cm^2)	$CSA_{max}2$: $CSA_{max}1$	Viable residual tumor (%)	Response classification
13	M	OS	R. distal femur	14.99	5.23	0.35	9.3	6.2	57.7	10.7	5.8	62.1	1.08	8	Good
14	M	OS	R. distal femur	11.99	1.53	0.13	10.0	7.5	75.0	7.4	5.1	37.7	0.50	5	Good
11	M	OS	R. proximal tibia	17.5	2.1	0.12	8.1	4.0	32.4	8.1	3.8	30.8	0.95	<2	Good
15	M	OS	R. proximal tibia	14	8.32	0.59	12.5	6.1	76.3	12.0	6.1	73.2	0.96	<5	Good
8	M	ES	R. proximal tibia	6.15	2.27	0.37	4.7	1.3	6.1	4.3	1.6	6.9	1.13	0	Good
15	M	ES	L. proximal tibia	26.1	2.46	0.09	NA[a]	NA	NA	NA	NA	NA	NA	0	Good
9	M	OS	L. distal femur	10.6	6.1	0.58	9.4	4.6	43.2	7.0	4.7	32.9	0.76	25	Poor
12	M	ES	R. proximal fibula	5.32	2.7	0.51	4.8	2.8	13.4	3.9	1.8	7.0	0.52	95	Poor

[a] Data not available

correlated to histological response, and should therefore not form the sole basis for decisions to escalate preoperative treatment [4]. FDG-PET/CT may become an accurate non-invasive test of response evaluation, analogous to current mid-treatment assessment in children with lymphoma [17].

FDG PET/CT combined with MRI in osteosarcoma has been demonstrated to be potentially useful in predicting histological response. It may therefore prove helpful for planning of surgery and tailoring of treatment [18]. The most important prognostic factor is tumor necrosis following neoadjuvant chemotherapy [19].

Early studies, predominantly adults with osteosarcoma and Ewing sarcoma, have looked at reduction in tumor/non-tumor tracer uptake before and after neo-adjuvant chemotherapy. These have showed promising results for FDG-PET in providing an accurate in vivo method for evaluating tumor response [20, 21]. We used SUV_{max} as the FDG-PET/CT parameter in our response assessment. SUV_{max} is more reliable than tumor-to-background ratios for semi-quantitative measurement of FDG-uptake and has low inter-observer variability in the characterization of sarcomas, which often demonstrate considerable heterogeneity in metabolic activity [22].

Our study raises the possibility, but does not confirm, that a high initial SUVmax may predict a better response. If true, then children with low initial tumor SUVmax would have a worse prognosis or be at higher risk of relapse. This finding conflicts were previous findings that sarcomas with higher pretherapy SUV_{max} had significantly poorer prognosis and that osteosarcomas with higher tumor/non-tumor uptake had poorer outcome [23, 24]. Both these studies were, however, primarily in adults.

A more recent study involving nine patients (five children) with osteosarcoma [25] showed a larger mean percent reduction in SUV_{max} after chemotherapy in patients with >90% necrosis compared to those with <10% necrosis: 74% reduced compared to 26% reduced, respectively. This supports our findings that the relative reduction in SUV_{max} (expressed in the current study as $SUV_{max}2$:$SUV_{max}1$ ratio and representing the proportion of metabolic activity remaining after chemotherapy) rather than the absolute value of SUV_{max} following chemotherapy may be a stronger predictor of tumor response. Using a cut-off point of $SUV_{max}2$:$SUV_{max}1<0.5$ to indicate a good response, Hamada et al. [25] determined the positive and negative predictive values were 80% and 100%, respectively, albeit with a very small dataset. Of the five children in this study, only one had poor response to therapy.

The largest study looking at response assessment in osteosarcoma by FDG-PET analysed 40 patients up to the age of 31 years (median, 15.1 years) with extremity tumors. Although they found that an SUV_{max} cut-off following chemotherapy of<2.5 was a significant predictor of im-

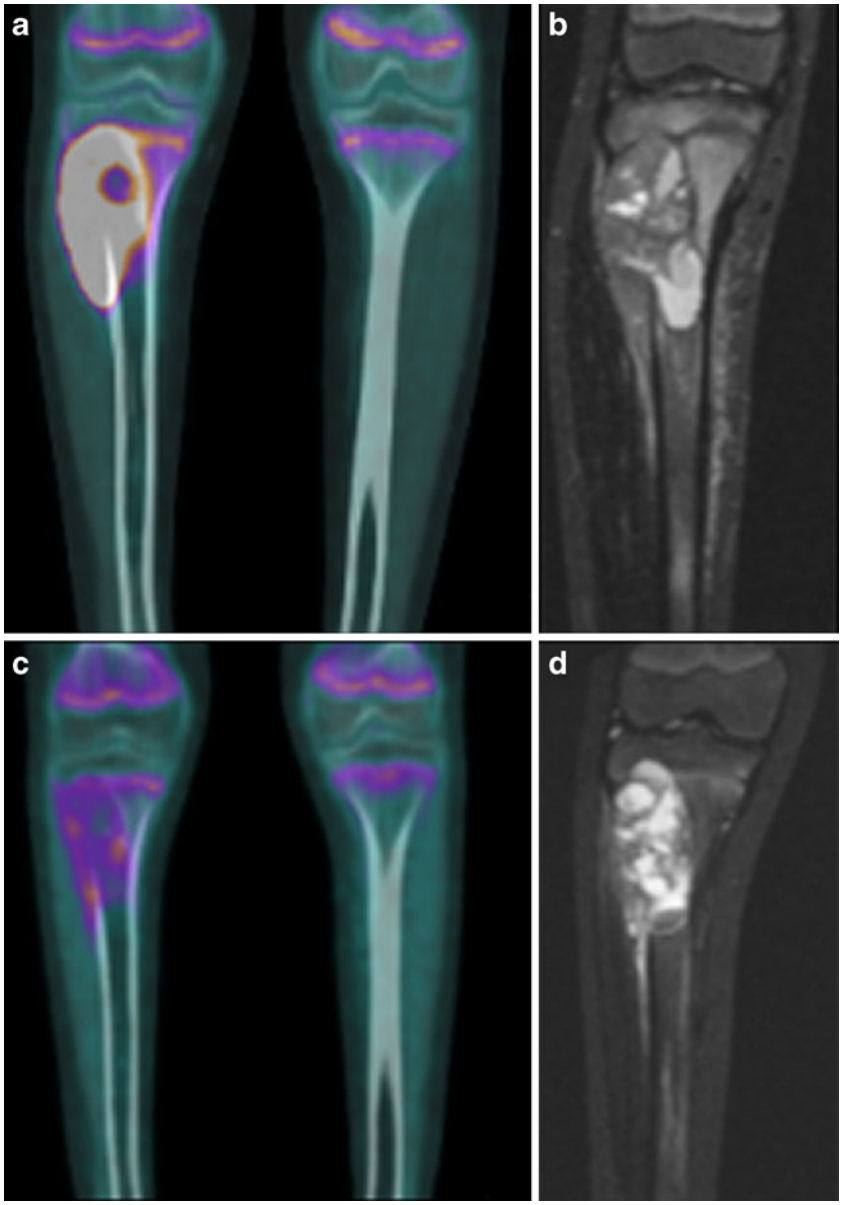

Fig. 4 Good histological tumor response in a 13-year-old male with OS involving the right proximal tibia. **a** Prior to therapy the PET/CT shows a markedly hypermetabolic tumor involving the right proximal tibia with $SUV_{max}1=17.5$. **b** The corresponding MRI at diagnosis showed an expansile, exophytic lesion in the lateral right proximal tibial metaphysis. **c** After chemotherapy, the PET/CT shows a marked reduction in tracer uptake with $SUV_{max}2=2.1$ and $SUV_{max}2$:$SUV_{max}1=0.12$, indicating a very good response. **d** MRI after chemotherapy showed a slight reduction in overall size, and gadolinium enhancement suggesting poor response. Histopathology revealed <2% viable cells confirming a good histological response to chemotherapy

proved outcome, there was only a weak correlation when using a cut-off of>50% reduction in SUV_{max} as a marker for good response (> 90% necrosis) [26]. The same group in an earlier study analysed 34 patients (up to 46 years old) with ES with similar findings [27]. The discrepancy in the effectiveness of relative reduction in SUV_{max} predicting tumor response between these reports and the study by Hamada et al. [25] may be due to a larger proportion of older patients in their cohorts.

Children with primary bone tumors probably constitute a biologically different group, distinct from adults, potentially rendering the translation of evidence from adult studies to pediatric practice invalid. Larger pediatric studies are warranted.

MRI has been shown previously to be accurate in the assessment of physeal tumor involvement [28]. Our review of six children supports this finding. Although we had a very small number of children in the comparison of PET/CT and CI, both modalities were very sensitive to detect physeal tumor involvement; however, MRI appeared to be more specific, with one false positive compared to two false positive results with PET/CT.

A major limitation of our study is the small number of eligible children included in the analysis, especially in the evaluation of tumor response parameters and assessment of physeal involvement. Correspondingly, there is overlap of the 95% confidence intervals in the measures of diagnostic test performance between PET/CT and CI; and the difference in the PET/CT and MRI parameters in predicting tumor response were not statistically significant. Larger studies with greater statistical power would be required to prove the trends seen in our study.

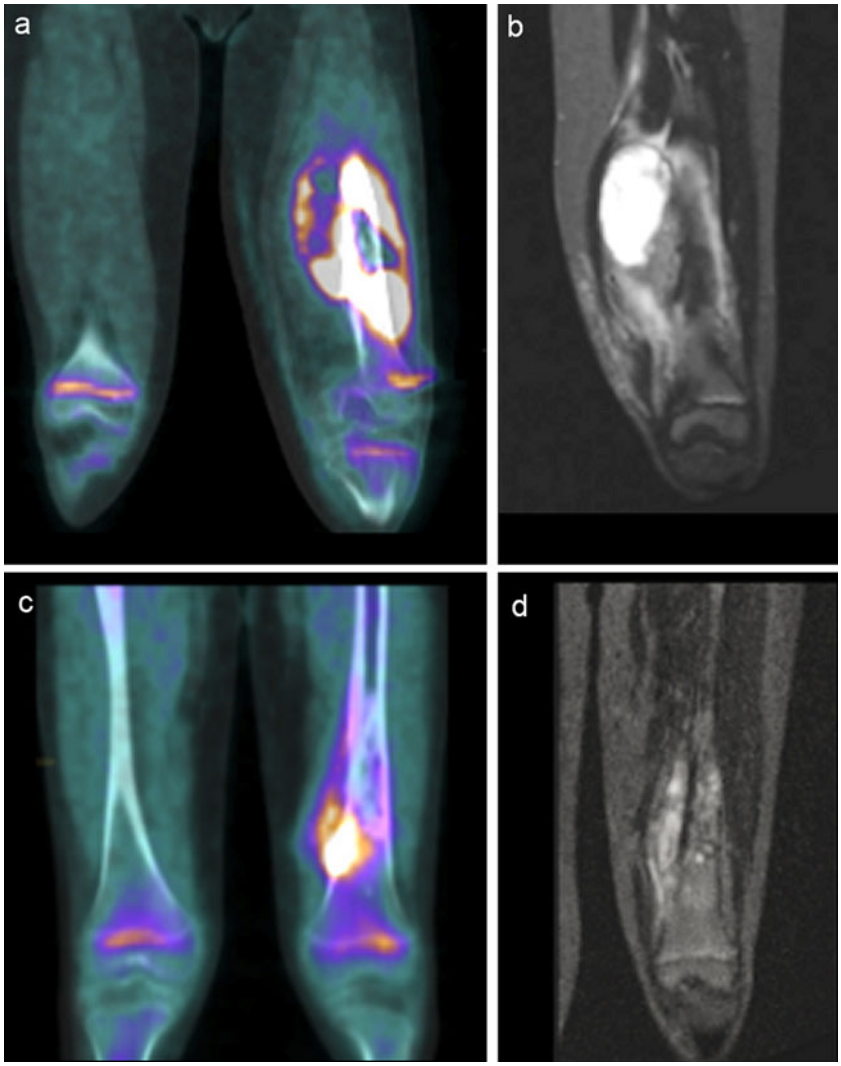

Fig. 5 Poor histological tumor response in an 11-year-old male with OS involving the distal left femur. **a** The staging PET/CT prior to therapy shows the tumor, demonstrating heterogeneous increased FDG uptake with $SUV_{max}1=10.6$. **b** The corresponding MRI shows a large soft tissue mass centred in the left vastus medialis muscle with periosteal reaction in the adjacent femur. It extends from the mid femur to the distal metaphyseal region with bone marrow involvement. **c** After chemotherapy, the PET/CT shows a significant reduction in the tumor extent and a persisting focal hypermetabolic region medially with $SUV_{max}2=6.1$ and $SUV_{max}2$:$SUV_{max}1=0.58$ indicating a poor response. **d** The MRI shows significant reduction in overall size and gadolinium enhancement of the tumor, suggesting good response. Histopathology after chemotherapy showed 25% viable malignant cells, confirming a poor histological response

The reports of both PET/CT and CI were generated with full knowledge of all other imaging and clinical information available at the time of the respective scan. There was the potential for the reported findings of one modality to bias the reporting of the other. A blinded re-assessment of all imaging may have produced more valid results but would not reflect everyday clinical practice.

For obvious ethical reasons, not all lesions detected in our study were biopsied. We therefore had to rely in part on (clinical) follow-up as a reference standard. This incorporated the change (resolution or progression) of each lesion as seen on follow-up imaging. The application of the reference standard is therefore not independent of the imaging modalities being evaluated, giving the potential for systematic reference standard misclassification. As this methodological limitation is unlikely to be satisfactorily solved, it is of particular importance that studies evaluating diagnostic performance clearly and thoroughly explain how

Table 7 PET/CT and MRI for detection of physeal involvement by metaphyseal tumors. *R* Right, *L* left

Metaphyseal tumor location	Physeal involvement on PET/CT	Physeal involvement on MRI	Physeal involvement on histology
R distal femur	Yes	Yes	Yes
R distal femur	Yes	Yes	Yes
L proximal tibia	Yes	Yes	Yes
R proximal tibia	Yes	Yes	Yes
R proximal tibia	Yes	Yes	No
R proximal fibula	Yes	No	No

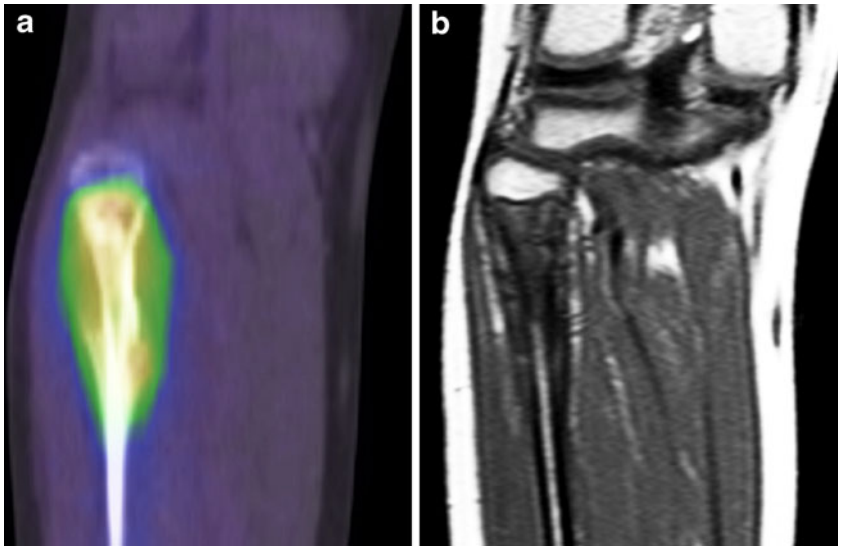

Fig. 6 Example of a PET false positive, MRI true negative for detecting epiphyseal involvement. The images were performed at diagnosis of a 12-year-old boy with right proximal fibular ES. **a** FDG PET/CT shows intense tracer uptake in the primary tumor appearing to breach the growth plate medially. **b** Corresponding MRI scan shows abnormal low signal in the tumor extending up to but not breaching the growth plate. Post operative histopathology did not show epiphyseal tumor involvement

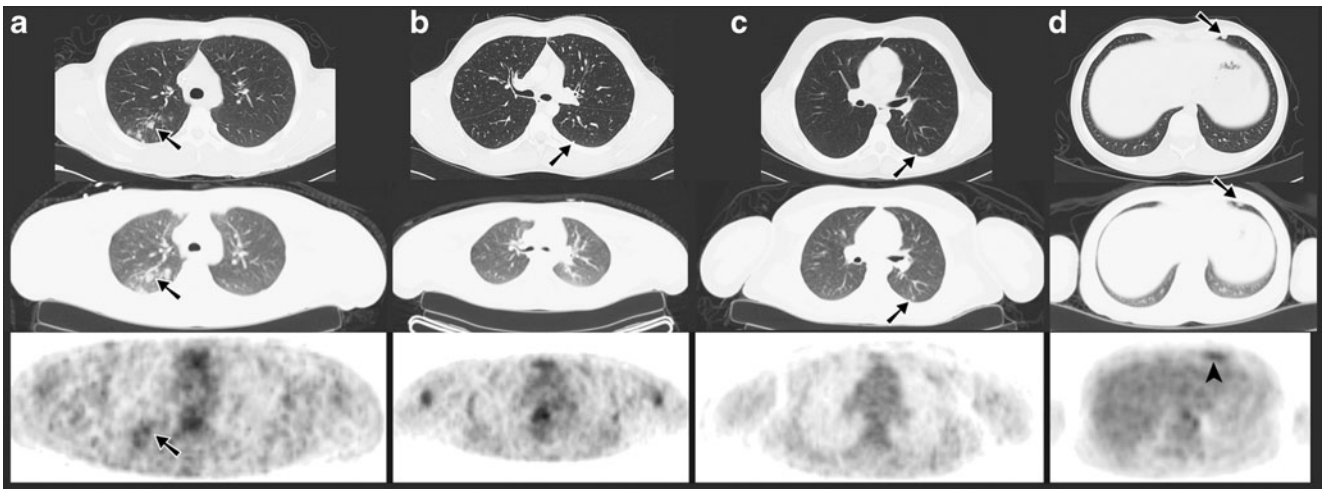

Fig. 7 Characterising lung lesions in children with primary bone tumors remains challenging on both FDG PET/CT and dedicated diagnostic CT. Four cases of lung lesions with variable findings on CI (diagnostic CT) and FDG PET/CT are presented (**a**–**d**). In each case the *upper image* is the diagnostic CT, the *middle image* is the low dose attenuation CT component of PET/CT, and the *lower image* is the corresponding attenuation corrected FDG PET. Note that the diagnostic CT studies were performed during an inspiratory breath hold with arms raised, while the FDG PET/CT was performed during normal tidal respiration with arms at the patient's side. **a** Concordant true positive lung lesions. At diagnosis, several nodular opacities were seen in the superior segment of the right lower lobe apparent on both the diagnostic CT (*arrow*) and the low dose attenuation CT component of the PET/CT (*arrow*) and demonstrated increased FDG uptake (*arrow*). **b** Discordant CI false positive lung lesion. At diagnosis, a 3-mm subpleural nodule was identified on diagnostic CT and considered suspicious for metastasis (*arrow*). The lesion was not apparent on either the low dose attenuation CT or FDG component of the PET/CT study. Diagnostic CT hookwire and thorascopic guided biopsy revealed a benign subpleural lymph node. **c** Concordant false positive lung lesions. During surveillance there was a new 5-mm nodule identified in the superior segment of the left lower lobe seen on both diagnostic CT (*arrow*) and the low dose attenuation CT component of the PET/CT (*arrow*). Although there was no apparent corresponding increase in FDG uptake, it was considered suspicious for recurrent malignancy. The lesion resolved on subsequent imaging without further cancer directed therapy and was regarded as a benign inflammatory nodule. **d** Discordant PET/CT false negative lung lesion. During surveillance, a new 7-mm sub-pleural nodule was identified in the anterior aspect of the left lower lobe on diagnostic CT (*arrow*). The lesion appeared more diffuse on the low-dose attenuation CT component of the PET/CT (*arrow*) without increased FDG uptake and was not identified as suspicious for recurrent metastasis. The lesion was proven by biopsy to be recurrent ES. The diffuse FDG accumulation seen in a location more medial to the lung lesion localised to physiologic brown fat (*open arrow*)

the reference standard (in addition to classification of a "positive" and "negative" scan result) is classified, as has been done in our report. In fact, there are suggested guidelines on the reporting of studies of diagnostic accuracy that should be adhered to wherever possible [29].

Conclusion

In children with primary bone tumors, PET/CT appears to be more sensitive and specific in evaluating lesions outside of the lungs. While less sensitive for detecting malignant lung lesions, the higher specificity of PET/CT renders it more useful than CI in confirming lung metastases when positive. On PET/CT, SUV_{max} reduction may be able to predict response to neo-adjuvant chemotherapy. Change in tumor size on MRI does not appear to be predictive of tumor response. Both PET/CT and MRI may be very sensitive but poorly specific in predicting physeal involvement of primary metaphyseal tumors.

Acknowledgments Supported in part by grants from the Dutch Cancer Society (C.S.) and from Department of Oncology, The Children's Hospital at Westmead, Sydney, Australia (K.L.).

References

1. Howman-Giles R, Hicks RJ, McCowage G et al (2006) Primary bone tumors. In: Charron M (ed) Practical pediatric PET imaging. Springer, New York
2. Bielack SS, Kempf-Bielack B, Delling G et al (2002) Prognostic factors in high-grade osteosarcoma of the extremities or trunk: an analysis of 1,702 patients treated on neoadjuvant cooperative osteosarcoma study group protocols. J Clin Oncol 20:776–790
3. Saifuddin A (2002) The accuracy of imaging in the local staging of appendicular osteosarcoma. Skeletal Radiol 31:191–201
4. Brisse H, Ollivier L, Edeline V et al (2004) Imaging of malignant tumours of the long bones in children: monitoring response to neoadjuvant chemotherapy and preoperative assessment. Pediatr Radiol 34:595–605
5. Bastiaannet E, Groen H, Jager PL et al (2004) The value of FDG-PET in the detection, grading and response to therapy of soft tissue and bone sarcomas; a systematic review and meta-analysis. Cancer Treat Rev 30:83–101
6. Franzius C, Daldrup-Link HE, Wagner-Bohn A et al (2002) FDG-PET for detection of recurrences from malignant primary bone tumors: comparison with conventional imaging. Ann Oncol 13:157–160
7. Bredella MA, Caputo GR, Steinbach LS et al (2002) Value of FDG positron emission tomography in conjunction with MR imaging for evaluating therapy response in patients with musculoskeletal sarcomas. AJR 179:1145–1150
8. Costelloe CM, Macapinlac HA, Madewell JE et al (2009) 18F-FDG PET/CT as an indicator of progression-free and overall survival in osteosarcoma. J Nucl Med 50:340–347
9. Schuetze SM, Rubin BP, Vernon C et al (2005) Use of positron emission tomography in localized extremity soft tissue sarcoma treated with neoadjuvant chemotherapy. Cancer 103:339–348
10. McCarville MB, Christie R, Daw NC et al (2005) PET/CT in the evaluation of childhood sarcomas. AJR 184:1293–1304
11. Volker T, Denecke T, Steffen I et al (2007) Positron emission tomography for staging of pediatric sarcoma patients: results of a prospective multicenter trial. J Clin Oncol 25:5435–5441
12. Lowrey R Clinical calculator 1. http://faculty.vassar.edu/lowry/clin1.html. Accessed November 2010
13. Franzius C, Daldrup-Link HE, Sciuk J et al (2001) FDG-PET for detection of pulmonary metastases from malignant primary bone tumors: comparison with spiral CT. Ann Oncol 12:479–486
14. Christensen JA, Nathan MA, Mullan BP et al (2006) Characterization of the solitary pulmonary nodule: 18F-FDG PET versus nodule-enhancement CT. AJR 187:1361–1367
15. Deeks JJ, Altman DG (2004) Diagnostic tests 4: likelihood ratios. BMJ 329:168–169
16. Peat J, Barton B (2005) In: Medical statistics: a guide to data analysis and critical appraisal, 1st edn. Blackwell, Malden, MA, pp 285–286
17. Furth C, Steffen IG, Amthauer H et al (2009) Early and late therapy response assessment with [18F]fluorodeoxyglucose positron emission tomography in pediatric Hodgkin's lymphoma: analysis of a prospective multicenter trial. J Clin Oncol 27:4385–4391
18. Cheon GJ, Kim MS, Lee JA et al (2009) Prediction model of chemotherapy response in osteosarcoma by 18F-FDG PET and MRI. J Nucl Med 50:1435–1440
19. Davis AM, Bell RS, Goodwin PJ (1994) Prognostic factors in osteosarcoma: a critical review. J Clin Oncol 12:423–431
20. Franzius C, Sciuk J, Brinkschmidt C et al (2000) Evaluation of chemotherapy response in primary bone tumors with F-18 FDG positron emission tomography compared with histologically assessed tumor necrosis. Clin Nucl Med 25:874–881
21. Schulte M, Brecht-Krauss D, Werner M et al (1999) Evaluation of neoadjuvant therapy response of osteogenic sarcoma using FDG PET. J Nucl Med 40:1637–1643
22. Benz MR, Evilevitch V, Allen-Auerbach MS et al (2008) Treatment monitoring by 18F-FDG PET/CT in patients with sarcomas: interobserver variability of quantitative parameters in treatment-induced changes in histopathologically responding and nonresponding tumors. J Nucl Med 49:1038–1046. doi:10.2967/jnumed.107.050187
23. Eary JF, O'Sullivan F, Powitan Y et al (2002) Sarcoma tumor FDG uptake measured by PET and patient outcome: a retrospective analysis. Eur J Nucl Med Mol Imaging 29:1149–1154
24. Franzius C, Bielack S, Flege S et al (2002) Prognostic significance of (18)F-FDG and (99 m)Tc-methylene diphosphonate uptake in primary osteosarcoma. J Nucl Med 43:1012–1017
25. Hamada K, Tomita Y, Inoue A et al (2009) Evaluation of chemotherapy response in osteosarcoma with FDG-PET. Ann Nucl Med 23:89–95
26. Hawkins DS, Conrad EU 3rd, Butrynski JE et al (2009) [F-^{18}]-fluorodeoxy-D-glucose-positron emission tomography response is associated with outcome for extremity osteosarcoma in children and young adults. Cancer 115:3519–3525
27. Hawkins DS, Schuetze SM, Butrynski JE et al (2005) [18F] Fluorodeoxyglucose positron emission tomography predicts outcome for Ewing sarcoma family of tumors. J Clin Oncol 23:8828–8834
28. Panuel M, Gentet JC, Scheiner C et al (1993) Physeal and epiphyseal extent of primary malignant bone tumors in childhood. Correlation of preoperative MRI and the pathologic examination. Pediatr Radiol 23:421–424
29. Bossuyt PM, Reitsma JB, Bruns DE et al (2003) Towards complete and accurate reporting of studies of diagnostic accuracy: the STARD initiative. Clin Radiol 58:575–580